



Utilizing real and statistically reconstructed microstructures for the viscoelastic modeling of polymer nanocomposites

Hua Deng^a, Yu Liu^{a,b}, Donghai Gai^a, Dmitriy A. Dikin^a, Karl W. Putz^a, Wei Chen^a,
L. Catherine Brinson^{a,c,*}, Craig Burkhart^d, Mike Poldneff^e, Bing Jiang^d, George J. Papakonstantopoulos^d

^a Department of Mechanical Engineering, Northwestern University, Evanston, IL 60208, USA

^b School of Mechatronics Engineering, University of Electronic Science and Technology of China, Chengdu, Sichuan 611731, PR China

^c Department of Materials Science and Engineering, Northwestern University, Evanston, IL 60208, USA

^d Global Materials Science Division, The Goodyear Tire & Rubber Company, 142 Goodyear Blvd., Akron, Ohio 44305, USA

^e External Science and Technology Division, The Goodyear Tire & Rubber Company, 200 Innovation Way, Akron, Ohio 44309, USA

ARTICLE INFO

Article history:

Received 22 September 2011

Received in revised form 20 February 2012

Accepted 21 March 2012

Available online 30 March 2012

Keywords:

C. Finite element analysis

A. Nano composites

B. Mechanical properties

Image analysis and reconstruction

ABSTRACT

In this paper, we present a new approach to finite element modeling of a nanoparticle filled polymer system that utilizes the actual and statistically reconstructed microstructures of the material. Typically, description of polymer nanocomposites for microstructure generation is difficult given the high degrees of freedom inherent in the location of each nanoparticle. The lack of true microstructure utilization hinders our ability to understand the interaction between the nanoparticle and polymer, which cannot easily be deconvoluted from experiments alone. We consider here a material system of carbon black particle fillers dispersed in synthetic natural rubber. Scanning Electron Microscope (SEM) images are first taken of these carbon black-rubber composites samples and then transformed into binary images. The binary images from either a microscope image of original specimens or microstructure reconstruction according to the material statistical description are used as geometric inputs for the finite element model along with experimentally determined viscoelastic properties of pure rubber. Simulations on the viscoelastic properties of the rubber composites are performed through ABAQUS. The simulated results are then compared with composite viscoelastic data in both frequency and temperature domains. The comparison shows that for the specific rubber/CB composite discussed in this paper, the thickness being 25 nm and relaxation time being 32 times that of matrix polymer provide the best approximations for the properties of interfacial polymer.

© 2012 Elsevier Ltd. All rights reserved.

1. Introduction

Polymer nanocomposites are materials composed of polymeric matrix in which inclusions (spheres, nanotubes, platelets) of nano-scale dimensions are incorporated. Polymer nanocomposites have been investigated for the past decade because of their outstanding material properties and great potential. The addition of nanosize inclusions into polymer matrix combines the advantage of polymer itself and the excellent properties of nanoparticles. Additionally, interactions between the nanofillers and the surrounding polymer chains alter the mobility of these polymer chains, resulting in a regime of “interphase” polymer, in which the material properties differ from the bulk matrix. Due to the high surface-to-volume ratio of nanofillers, the effects of this special region play an important role in the overall properties of nanocomposites, especially

viscoelastic responses [1–4]. The composite material composition and properties are highly tunable, and performance improvements are currently demonstrated for a wide range of properties including stiffness, strength, heat resistance, optical properties, electric conductivity and barrier properties [5–11], leading to a wide range of applications in vehicle, aerospace, medical device industries [12–15].

At the same time, the sensitivity of final nanocomposite properties to small changes in processing, functionalization, additives, and volume fraction has made development of these materials difficult. Much of the property sensitivity can be linked to two factors: (1) changes in dispersion/distribution of nanoparticles and (2) chemical interaction differences between particle surfaces and matrix polymer. Both of these factors affect the properties, extent, and connectivity of interphase domains in the composite system. Therefore, development of methods which can directly link nanoparticle morphology to properties are valuable toward fundamental understanding of the underlying physics, as well as for facilitating material design. This paper deals directly with this needed research.

* Corresponding author at: Department of Mechanical Engineering, Northwestern University, Evanston, IL 60208, USA. Tel.: +1 847 467 2347.

E-mail address: cbrinson@northwestern.edu (L. Catherine Brinson).

Many modeling frameworks have been developed to explain the material properties of polymer composites with nanofillers. These include methods at both nanoscale (molecular dynamics [16–21]) and micro/macro scale (continuum theories [22–24]). Although MD simulations are able to capture the configurations of polymer chains and particles embedded at nanoscale, they could only account for structures with small number of particles and limited polymer chains due to the computational constraints. To study the mechanical responses of polymer nanocomposites at micro/macro scale level, many continuum models have been developed, including rule-of-mixture, self-consistent scheme [25–27], Mori–Tanaka method [28], etc. However, these methods do not explicitly consider spatial distribution of nanoparticles.

The finite element method is another continuum model that has been widely used to predict the viscoelastic properties of polymer nanocomposite systems [29–31]. Recently Qiao and Brinson [32,33] developed a 2D plain strain finite element model to study the impact of interphase on the viscoelastic properties as well as thermal response of polymeric nanocomposites. In this model, finite element analysis is performed on a representative volume element (RVE) with periodic structure (inhomogeneous distribution of particles inside a unit square). Their results show that the distribution of particles has a significant impact on the interphase percolation and further influence on the viscoelastic properties of the bulk composites.

Among the various kinds of polymer nanocomposites, carbon-black/rubber composites is one of the most commonly used materials worldwide in communication, transportation, architecture industries [34]. The creep and relaxation behaviors of carbon black filled rubber systems have been received increasing attention recently [35–38]. Constitutive models [39,40] attempting to characterize their viscoelastic behaviors are also developed for large deformations. Montes and White [41] presented a rheological model to distinct composites with low interaction (viscoelastic) and high interaction ('thixotropic-plastic-viscoelastic') between rubber and carbon black particles. The morphology of carbon black dispersed in rubber is a challenge in predicting the mechanical behaviors of the composites.

In this work, we built up a microstructural image-based finite element framework to simulate and predict linear viscoelastic mechanical responses of carbon black-rubber composites. We focus on detailed characterization of the microstructure morphology which has twofold benefits. First, it enables a quantitative understanding of the microstructure–property relationship and the sensitivity of various descriptors of microstructure morphology, such as clustering, percolation, dispersion, and orientation of inclusions, with respect to their impacts on the prediction of bulk properties [42,43]. The knowledge gained from this can be further utilized for sophisticated material design through shaping the microstructure morphology via controlling ingredients and manufacturing processes [42,43]. Second, based on the statistical descriptors, a microstructure can be reconstructed from a sample space to reduce the need for difficult and time consuming high resolution imaging techniques like scanning or transmission electron microscopy (SEM, TEM). In the situation where three dimensional (3D) imaging like X-ray microtomography technique is not affordable or unavailable and information about the isotropy of the material is known, the 3D structure of heterogeneous material can be reconstructed using statistical information extracted from 2D planar cuts and extrapolated to the third dimension [42–47]. To predict the material property of a given microstructure, the binary digitized medium from either the real microscopic image of specimens or microstructure reconstruction are imported into ABAQUS input file as the geometries of the finite element model. The predicted $\tan \delta$ curves of the composites are compared with experimental $\tan \delta$ curves from DMA (Dynamic Mechanical Analysis) tests. Due to

the complexity of retrieving interphase properties from experiments, the unknown interphase properties can be extracted by calibration to best fit the experimental results.

2. Modeling framework

2.1. Data-driven framework for microstructure construction

A data-driven framework was developed to generate binary digitized medium from the grey SEM image [48]. It includes five steps as shown in Fig. 1. The grayscale microstructure images are taken by a high-resolution imaging technique (SEM shown in Fig. 1) in Step 1 and act as the data driving the rest of the process.

For two-phase materials like the carbon black filled rubber composite, Step 2 transforms a high-resolution grayscale image to a binary image that discretely separates the two phases. Two image enhancement algorithms, namely the contrast-adjustment method and the median noise filtering algorithm, are first used to increase the quality and contrast of the grayscale images before transformation [49]. The known volume fraction of the experimental samples are used as the threshold criteria for determining white and black pixel populations.

In step 3 we characterize the microstructure morphology with a set of statistical descriptors based on the binary digitized medium. A variety of descriptors have been proposed to quantify the inherent statistical characteristic of material microstructure [50–54]. Two point correlation function $S_2(r)$ and two-point cluster correlation function $C_2(r)$, defined as the probability of finding a pair of points in the same phase and the probability of finding a pair of point in the same cluster respectively, are chosen to characterize the carbon black filled rubber composite in our study [55,56]. An illustration of the two-point correlation and two-point cluster correlation of a polymer composite with 20% carbon black fillers is shown in Fig. 2.

Given the statistical descriptors from the real micro structural image, i.e., two-point correlation and two-point cluster correlation, the microstructure can be reconstructed in a statistical sense. In Step 4, the microstructure reconstruction is naturally formulated as an optimization problem where the discrepancies between the target statistical descriptors and that of a reconstructed image are minimized [46,47,55,50,57,58]. The simulated annealing algorithm is developed to resolve the resulting optimization problem [46,47,56], and to find the "optimal" material configuration based on thousands of microstructures generated in a stochastic fashion. The detailed procedures of the optimization can be found in [48]. Many such statistically equivalent microstructures can be generated through Step 4. Then in Step 5, the binary digitized medium from either the real microscopic image of specimens or microstructure reconstruction will be imported into ABAQUS as the geometries. An example of the comparison between the original image and reconstructed images is shown in Fig. 3.

2.2. 2D Finite element simulation

We adopted a 2D plain stress finite element model to predict the $\tan \delta$ curve of carbon black filled rubber composites and compare with experimental data. The discretization of a 2D binary image directly retrieved from either the SEM image of rubber-carbon black composite sample or statistical microstructure reconstruction is used as one input geometry into our FE model (Fig. 4). In this process, the image with its physical size $7.46 \mu\text{m} \times 7.46 \mu\text{m}$ is divided into 300×300 pixels, where each pixel has the initial material properties of either carbon black or the matrix, depending on the color (black or white) of the pixel in the image. Therefore the pixels belonging to particle phase correspond to carbon black

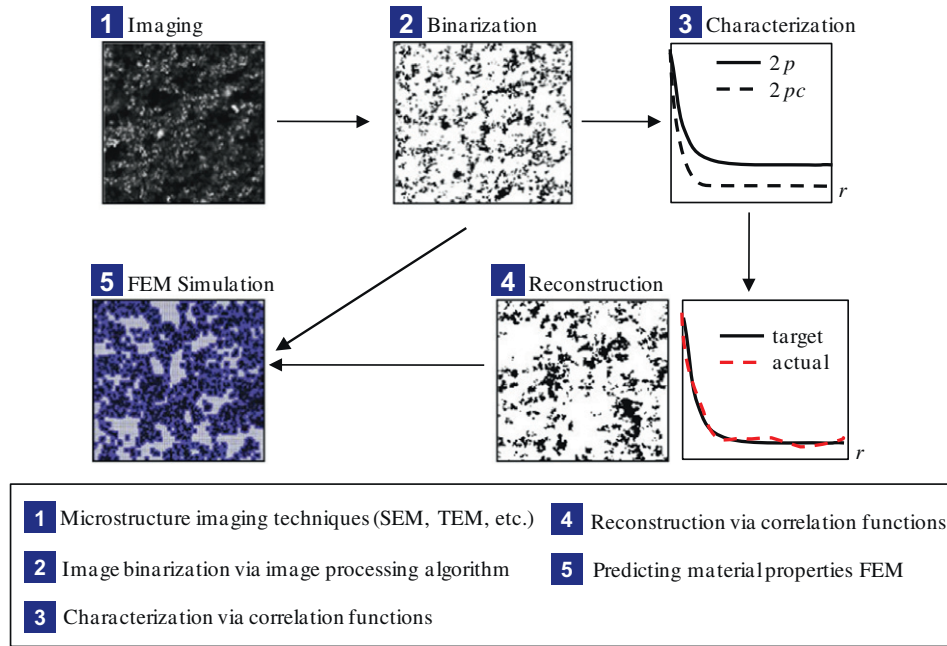


Fig. 1. The Basic Framework of Data-Driven Modeling Methods (“target” refers to the correlations of the digitized medium, “actual” are the correlations of reconstructed material).

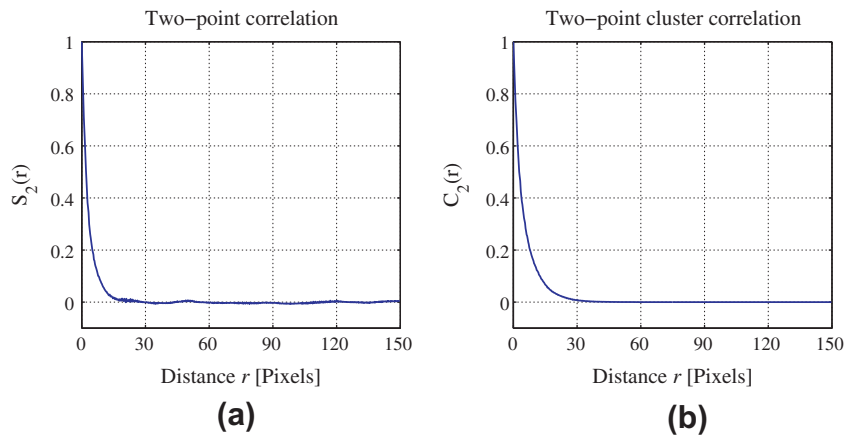


Fig. 2. An illustration of correlation functions for a sample with 20% carbon black filler. (a) The two-point correlation function S_2 ; (b) The two-point cluster correlation C_2 . (r = distance in pixels).

nanoparticles with the diameter 25 nm. Calculations are then performed on the experimentally defined material geometry and on statistically equivalent geometries. The results of the ABAQUS simulations can be compared to understand the effectiveness of the statistical reconstruction. We chose the RVE size as 300×300 because we found this was the minimum size that could give us a convergent material response.

To consider the influence of interphase polymer on the effective properties, multiple layers of interphase pixels are added surrounding the carbon black pixels into the image, in order to define the interphase region. Each pixel corresponds to a 4 noded plane stress quadrilateral element in the model (see Fig. 5).

2.3. Material parameters: DMA tests and mastercurve construction

From Dynamic Mechanical Analysis (DMA), we can obtain the storage and loss moduli of neat rubber and carbon black filled samples in both temperature and frequency domain. Fig. 6a shows the change of $\tan \delta$ with temperature at the frequency 11 Hz. The

Time-Temperature-Superposition-Principle (TTSP) is used to trade off temperature for time and to combine mechanical tests of practical duration at multiple temperatures to determine the frequency dependent properties [59]. The combined curve is called the mastercurve. Fig. 6b shows the mastercurves of neat rubber (SNR) and composites (SNR-C5) samples. This frequency response of neat rubber is then used as the input of the matrix properties in this FE model, while the composite mastercurve is used for comparison with the simulated results from the ABAQUS model. It is clearly shown that the $\tan \delta$ curve has been broadened in both frequency and temperature domain due to the nanofiller reinforcement. Also the $\tan \delta$ peak of composites shifts towards higher temperature (lower frequency) compared with that of the neat rubber. It is to be noted that for the purpose of comparison, each curve is normalized at its maximum value and thus has the peak at 1.

In the simulation, the volume fraction of carbon black in the rubber composite is 20%. The carbon black particles are regarded as elastic with the instantaneous Young’s modulus 100 GPa and Poisson’s ratio 0.4. The properties of the interphase (polymer with

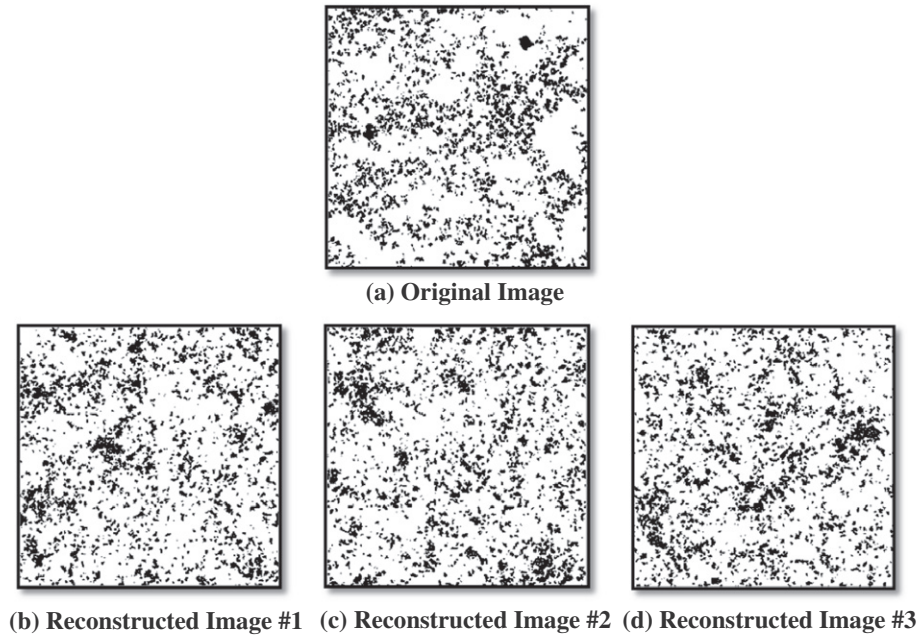


Fig. 3. An example of an original image and its reconstructed images.

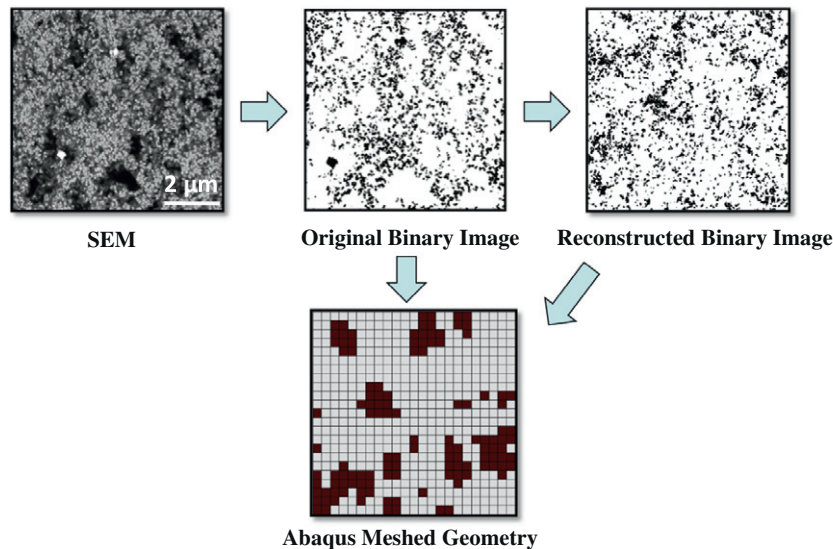


Fig. 4. Method to obtain finite element simulations on microstructure: transform SEM image to binary image, compute statistical equivalent reconstructed binary image, discretize images into meshes and solve for effective response in ABAQUS. Image shown is 20% carbon black. The meshed image shows only portion of the whole geometry.

altered properties) are regarded as related to those of the bulk polymer matrix by a simply shift in the frequency domain towards lower frequency (Fig. 7), representing an attractive interaction between the polymer and the filler. The extent of interphase and the amount of shift will be tuned in the last step of the analysis with aim of determining the optimal properties and domain size which enable the predicted curve from finite element simulation to best fit with the experimental curve.

3. Results and discussion

3.1. Images and statistical replicas

To illustrate that the proposed statistical descriptors, i.e., two-point correlation and two-point cluster correlation, adequately represent the microstructure for reconstruction, the finite element

simulation results for both the original and several reconstructions are plotted in Fig. 8. As observed from Fig. 8, the reconstructed digitized microstructure has almost the same material behavior prediction with that using the original digitized medium. As the volume fraction of interphase increases with thicker interphase layers, the $\tan \delta$ peak shifts from being dominated by matrix polymer $\tan \delta$ to being dominated by interphase polymer. Geometric percolation of interphase occurs when interphase thickness is equal to twice of pixel size in both the original and reconstructed images. Some discrepancies between the magnitude of the $\tan \delta$ are observed in the less percolated cases due to differences in the extent of the percolation with different geometries. However, the location of the $\tan \delta$ peak is nearly identical for all cases except for the one when percolation occurs (thickness = 2). Thus, the reconstructed images provide a qualitatively reasonable prediction of the composite material viscoelastic response.

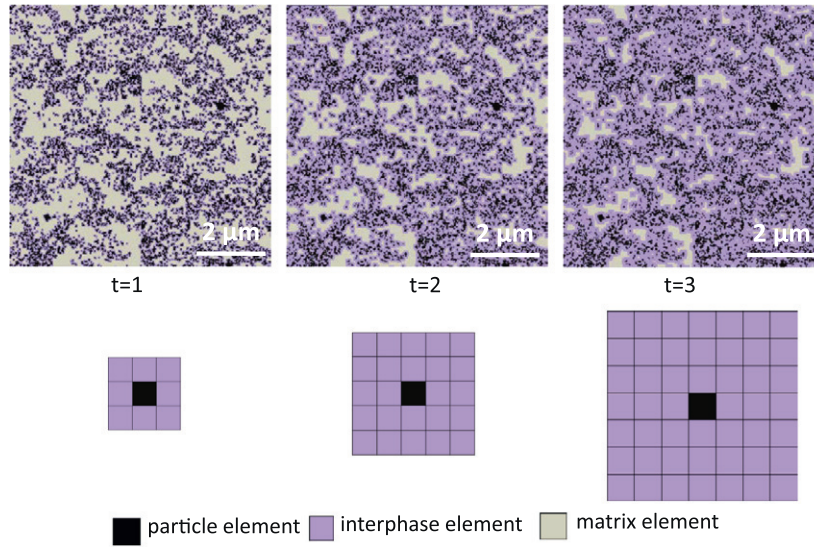


Fig. 5. Incorporating interphase zones of different extent into a given microstructural RVE. One to three layers of interphase pixels surrounding the carbon black particles.

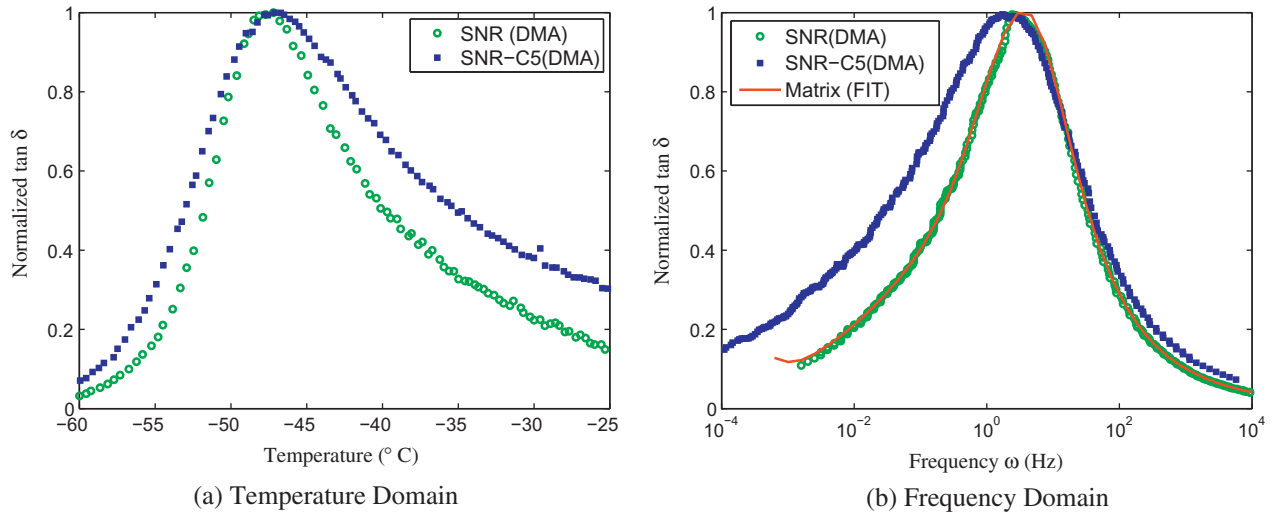


Fig. 6. Experimental DMA data of normalized $\tan \delta$ in both temperature domain and frequency domain, the latter obtained via TTSP. The frequency response of SNR matrix was then fit by Prony Series which can be imported into ABAQUS.

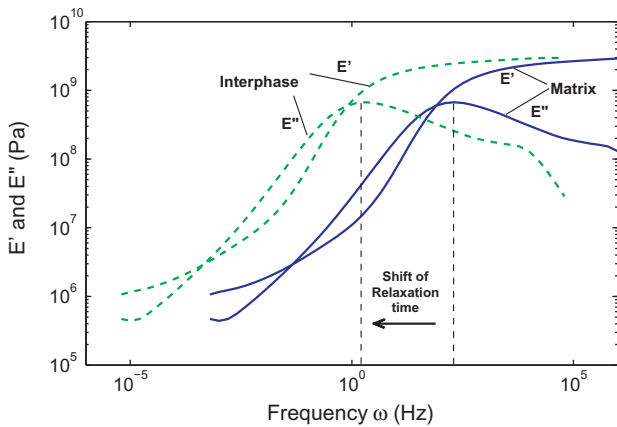


Fig. 7. Relation of material properties between interphase and bulk matrix by a simple shift in frequency/time space representing increase of relaxation times in the interphase domain relative to the matrix polymer.

3.2. Finite element simulation results and comparison to experiment

To compare with the experimental data of the rubber-carbon black composites, both frequency and temperature response simulations were performed with the above 2D FE model. Direct Steady State Dynamic analysis is performed to simulate the frequency response of the rubber composites. To simulate the temperature domain response, models at various temperatures are generated by altering Prony Series coefficients for matrix and interphase using the shift factors obtained from the process of mastercurve construction via TTSP. Simulations of these models at different temperatures are then performed at a fixed frequency point, to ultimately produce a temperature-sweep simulation curve at a given frequency. Since experimental determination of local interphase properties remains challenging [60], the simulations together with composite experimental data provide a way to solve an inverse problem to determine possible interphase properties. Although there are many parameters about the interphase properties (density, thickness, relaxation time, stiffness, glass transition time), the thickness and relaxation times are found to have

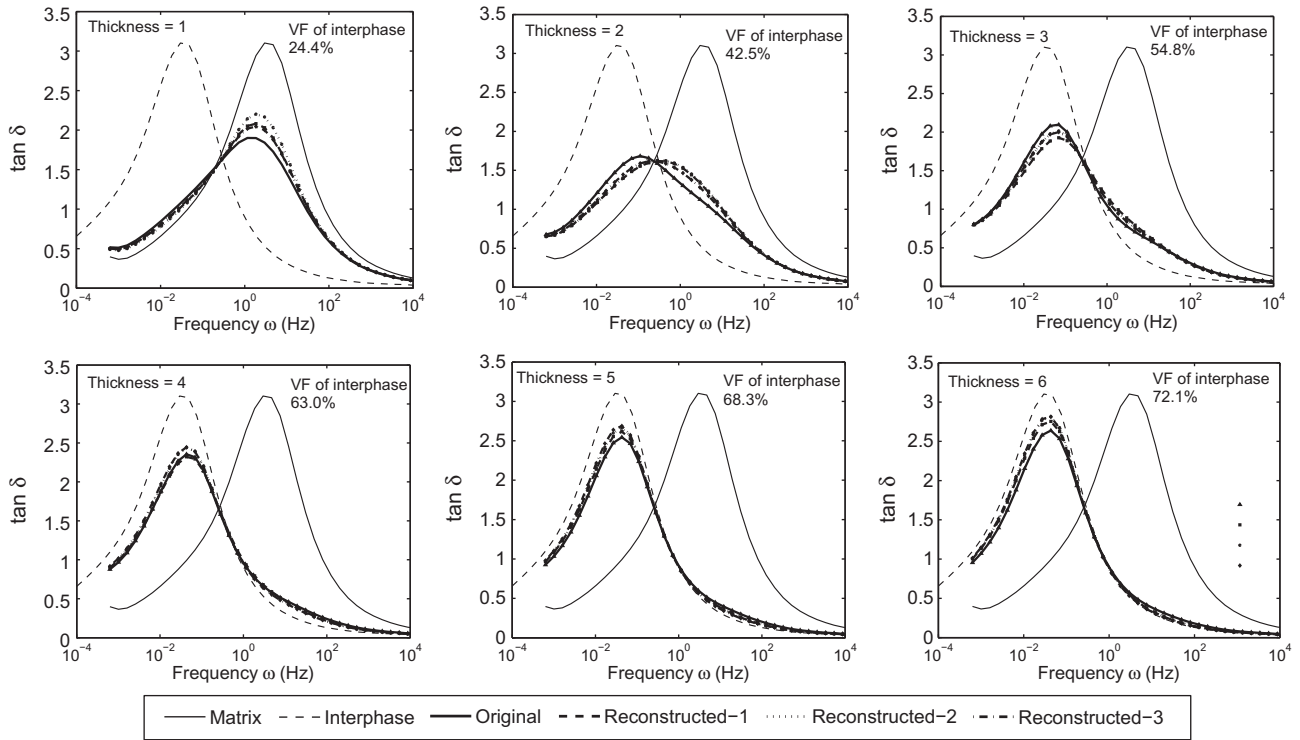


Fig. 8. The $\tan \delta$ response computed from the original and the reconstructed digitized medium with different setting of thickness of interphase layer.

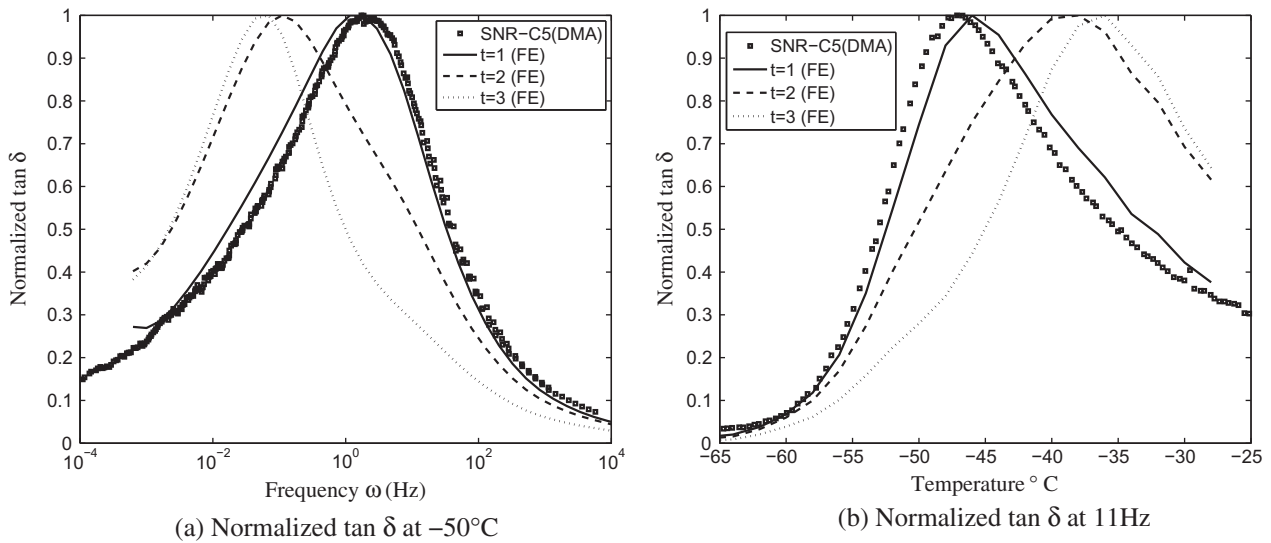


Fig. 9. Comparison of predicted $\tan \delta$ curves with experimental data: here the interphase properties are fixed while the interphase thickness is varied.

dominant impacts on the composite properties. It is known from literature on polymer thin films that the relaxation times are significantly altered near an attractive or repulsive substrate, demonstrated by significant changes in glass transition temperature [61–63]. Thus, here we change the thickness (number of pixels) and the relaxation times (decades of shift as indicated in Fig. 7) of the interphase, to study their effects on the $\tan \delta$ curve of the composites.

From experimental observations, the range of influence of nanoparticle reinforcement on the polymer chains can be as large as tens of nanometers. Thus we model the interphase region with the thickness from 1 to 3 pixel layers (25–75 nm) and set the

decades of shift (D_s) as 2.0 (see Fig. 9). It is to be noted that uniform properties are assigned through the interphase regime. Again for the purpose of comparison, each $\tan \delta (E''/E)$ curve is normalized at its maximum value. The results show that modeling the interphase region by one layer of pixel (~ 25 nm) provides the best match between the simulated curves and the experimental curve. Therefore $t = 1$ is chosen as the default value of interphase thickness, and we further vary the value of D_s from 0.5 decade to 2.0 decades). The simulation results indicate that assuming interphase properties shifted 1.5 decades toward lower frequencies from the matrix master curve, fit the experimental curve best (Fig. 10).

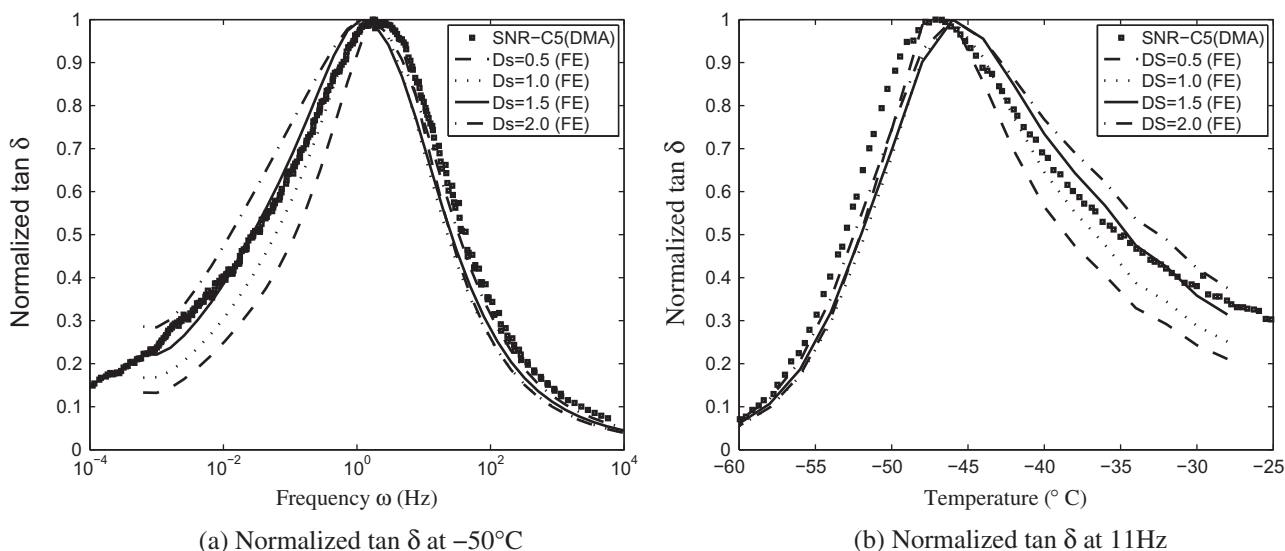


Fig. 10. Comparison of predicted $\tan \delta$ curves against experimental data: here the interphase thickness is fixed while the interphase properties, decades of shift (D_s), varied. Increasing D_s indicates increasingly longer relaxation times for the interphase.

From Figs. 9 and 10 we observe that the location of the $\tan \delta$ peak and the increase in breadth is well captured by the model with optimized interphase parameters. While this exercise does not provide a unique definitive solution for interphase, it does provide a reasonable set of properties that can extend our understanding of the interphase regime. In this case, the results indicate that the interphase zone is around 20 nm in extent with relaxation time approximately $10^{1.5}$ (~ 32) times that of the matrix polymer. Application of this method to similar material systems with changes in interaction chemistry may enhance our understanding of the impact of those chemical changes on interphase properties and extent.

4. Conclusion

We present an image based finite element approach to model heterogeneous materials. The viscoelastic responses ($\tan \delta$) of rubber/carbon black composites are simulated and compared with experimental data. SEM images of rubber/CB samples are first digitized and used as the original microstructure of the finite element geometry. Based on this original microstructure, statistical characterization is performed on and reconstructed microstructures with equivalent statistical information are generated. The proposed microstructure characterization and reconstruction process are validated through the comparison of the predicted material properties between simulations on original microscope images and reconstructed microstructure from the statistical descriptors of the original microscope images. This validation implies that it is then valid to use statistically created microstructures in order to probe the design space of new materials, which have not yet been made and therefore for which no SEM images yet exist. Using experimental data on the composite, by optimizing the extent and properties of interphase domain, the proposed finite element model provides a qualitative match between the predicted $\tan \delta$ curve and the experimental data. This method allows for extraction of viscoelastic properties of the interphase that are not possible through microstructures that are not based on the actual samples.

Acknowledgment

The authors thank the support of Goodyear Tire & Rubber Company.

References

- [1] Ramanathan T, Abdala AA, Stankovich S, Dikin DA, Herrera-Alonso M, Piner ADH, et al. Functionalized graphene sheets for polymer nanocomposites. *Nature Nanotechnology* 2008;3:327–31.
- [2] Schadler L, Brinson L, Sawyer WG. Polymer nanocomposites: a small part of the story. *J Miner, Met Mater Soc* 2007;59(3):53–60.
- [3] Ramanathan T, Liu H, Brinson LC. Functionalized swnt/polymer nanocomposites for dramatic property improvement. *J Polym Sci Part B – Polym Phys* 2005;43(17):2269–79.
- [4] Putz KW, Mitchell CA, Krishnamoorti R, Green PF. Elastic modulus of single-walled carbon nanotube/poly(methyl methacrylate) nanocomposites. *J Polym Sci Part B – Polym Phys* 2004;42(12):2286–93.
- [5] Cadek M, Coleman JN, Barron V, Hedicke K, Blau WJ. Morphological and mechanical properties of carbon-nanotube-reinforced semicrystalline and amorphous polymer composites. *Appl Phys Lett* 2002;81(27):5123–5.
- [6] Biercuk MJ, Llaguno MC, Radosavljevic M, Hyun JK, Johnson AT. Carbon nanotube composites for thermal management. *Appl Phys Lett* 2002;80(15):2767–9.
- [7] Cho J, Daniel IM. Reinforcement of carbon/epoxy composites with multiwall carbon nanotubes and dispersion enhancing block copolymers. *Scripta Mater* 2008;58:533–6.
- [8] Coleman JN, Khan U, Gun'ko YK. Mechanical reinforcement of polymers using carbon nanotubes. *Adv Mater* 2006;18(6):689–706.
- [9] Du F, Scogna RC, Zhou W, Brand S, Fischer JE, Winey KI. Nanotube networks in polymer nanocomposites: rheology and electrical conductivity. *Macromolecules* 2004;37(24):9048–55.
- [10] Rong MZ, Zhang MQ, Zheng YX, Zeng HM, Friedrich K. Improvement of tensile properties of nano-sio2/pp composites in relation to percolation mechanism. *Polymer* 2001;42(7):3301–4.
- [11] Sandler J, Shaffer MSP, Prasse T, Bauhofer W, Schulte K, Windle AH. Development of a dispersion process for carbon nanotubes in an epoxy matrix and the resulting electrical properties. *Polymer* 1999;40(21):5967–71.
- [12] Hussain F, Hojjati M, Okamoto M, Gorga RE. Review article: polymer-matrix nanocomposites, processing, manufacturing, and application: an overview. *J Compos Mater* 2006;40:1511–75.
- [13] Chou T-W, Gao L, Thostenson ET, Zhang Z, Byun J-H. An assessment of the science and technology of carbon nanotube-based fibers and composites. *Compos Sci Technol* 2010;70:1C19.
- [14] Winey KI, Vaia RA. Polymer nanocomposites. *MRS Bull* 2007;32:314–9.
- [15] Tjong S. Structural and mechanical properties of polymer nanocomposites. *Mater Sci Eng R* 2006;53:73–197.
- [16] Odegard G, Gates TS, Wise KE, Park C, Siochi EJ. Constitutive modeling of nanotube-reinforced polymer composites. *Compos Sci Technol* 2003;63(11):1671–87.
- [17] Odegard GM. Constitutive modeling of piezoelectric polymer composites. *Acta Mater* 2004;52(18):5315–30.
- [18] Smith GD, Bedrov D, Li L, Bytner O. A molecular dynamics simulation study of the viscoelastic properties of polymer nanocomposites. *J Chem Phys* 2002;117(20):9478–89.
- [19] Smith JS, Bedrov D, Smith GD. A molecular dynamics simulation study of nanoparticle interactions in a model polymer-nanoparticle composite. *Compos Sci Technol* 2003;63(11):1599–605.

- [20] Starr FW, Schroer TB, Glotzer SC. Molecular dynamics simulation of a polymer melt with a nanoscopic particle. *Macromolecules* 2002;35(11):4481–92.
- [21] Brown D, Marcadon V, Mi P, Albrold ND. Effect of filler particle size on the properties of model nanocomposites. *Macromolecules* 2008;41(4):1499–511.
- [22] Sheng N, Boyce MC, Parks DM, Rutledge GC, Abes JL, Cohen RE. Multiscale micromechanical modeling of polymer/clay nanocomposites and the effective clay particle. *Polymer* 2004;45(2):487–506.
- [23] Seidel GD, Lagoudas DC. Micromechanical analysis of the effective elastic properties of carbon nanotube reinforced composites. *Mech Mater* 2006;38(8–10):884–907.
- [24] Gao XL, Li K. A shear-lag model for carbon nanotube-reinforced polymer composites. *Int J Solids Struct* 2005;42(5–6):1649–67.
- [25] Alberola ND, Mele P. Interface and mechanical coupling effects in model particulate composites. *Polym Eng Sci* 1997;37(10):1712–21.
- [26] Hashin Z, Monteiro PJM. An inverse method to determine the elastic properties of the interphase between the aggregate and the cement paste. *Cement Concrete Res* 2002;32(8):1291–300.
- [27] Dickie RA. Heterogeneous polymer-polymer composites. i. theory of viscoelastic properties and equivalent mechanical models. *J Appl Polym Sci* 1973;17(1):45–63.
- [28] Mori T, Tanaka K. Average stress in matrix and average elastic energy of materials with misfitting inclusions. *Acta Metallurgica* 1973;21(5):571–4.
- [29] Wang HW, Zhou HW, Peng RD, LM Jr. Nanoreinforced polymer composites: 3d fem modeling with effective interface concept. *Compos Sci Technol* 2011;71(7):980–988.
- [30] Liu YJ, Chen XL. Evaluations of the effective material properties of carbon nanotube-based composites using a nanoscale representative volume element. *Mech Mater* 2003;35(1–2):69–81.
- [31] Song YS, Youn JR. Modeling of effective elastic properties for polymer based carbon nanotube composites. *Polymer* 2006;47(5):1741–8.
- [32] Qiao R, Brinson LC. Simulation of interphase percolation and gradients in polymer nanocomposites. *Compos Sci Technol* 2009;69(3–4):491–9.
- [33] Qiao R, Deng H, Putz K, Brinson LC. Effect of particle agglomeration and interphase on the glass transition temperature of polymer nanocomposites. *J Polym Sci Part B: Polym Phys* 2011;49(10):740–8.
- [34] Saritha A, Joseph K, Thomas S. Design, development and testing of rubber nanocomposites. *Trends Compos Mater Des Book Series: Key Eng Mater* 2010;425:61–93. <http://dx.doi.org/10.4028/www.scientific.net/KEM.425.61>
- [35] Oono R. Stress relaxation in carbon-black-filled styrene-butadiene rubber. *J Polym Sci Part B: Polym Phys* 1974;12:1383–94.
- [36] MacKenzie CI, Scanlan J. Stress relaxation in carbon-black-filled rubber vulcanizates at moderate strains. *Polymer* 1984;25(4):559–68.
- [37] Le HH, Ilich S, Radosch HJ. Characterization of the effect of the filler dispersion on the stress relaxation behavior of carbon black filled rubber composites. *Polymer* 2009;50(10):2294–303.
- [38] Mostafa A, Abouel-Kasem A, Bayoumi MR, El-Sebaie M. On the influence of cb loading on the creep and relaxation behavior of sbr and nbr rubber vulcanizates. *Mater Des* 2009;30(7):2721–5.
- [39] Abu-Abdeen M. Single and double-step stress relaxation and constitutive modeling of viscoelastic behavior of swelled and un-swelled natural rubber loaded with carbon black. *Mater Des* 2010;31(4):2078–84.
- [40] Bergstrom JS, Boyce MC. Constitutive modeling of the large strain time-dependent behavior of elastomers. *J Mech Phys Solids* 1998;46(5):931–54.
- [41] Montes S, White JL. Rheological models of rubber-carbon black compounds: low interaction viscoelastic models and high interaction thixotropic-plastic-viscoelastic models. *J Non-Newton Fluid Mech* 1993;49:277–98.
- [42] Fullwood DT, Niezgodá SR, Kalidindi SR. Microstructure reconstructions from 2-point statistics using phase-recovery algorithms. *Acta Mater* 2008;56(5):942–8.
- [43] Saheli G, Garmestani H, Adams BL. Microstructure design of a two phase composite using two-point correlation functions. *J Comput-Aided Mater Des* 2004;11(2–3):103–15.
- [44] Jiao Y, Stillinger S, Torquato FH. Modeling heterogeneous materials via two-point correlation functions: basic principles. *Phys Rev E* 2007;76(3):031110.
- [45] Jiao Y, Stillinger FH, Torquato S. Modeling heterogeneous materials via two-point correlation functions. ii. algorithmic details and applications. *Phys Rev E* 2008;77(3):031135.
- [46] Yeong CLY, Torquato S. Reconstructing random media. *Phys Rev E* 1998;57(1):495–506.
- [47] Yeong CLY, Torquato S. Reconstructing random media. ii. three-dimensional media from two-dimensional cuts. *Phys Rev E* 1998;58(1):224–33.
- [48] Liu Y, Greene MS, Chen W, Dikin DA, Liu WK. Microstructure reconstruction for stochastic multiscale material design. In: *ASME 2011 international design engineering technical conferences and computers and information in engineering conference*. Washington, DC, USA; 2011.
- [49] Abb F, Chermant L, Coster M, Gomina M, Chermant JL. Morphological characterization of ceramic-ceramic composites by image analysis. *Compos Sci Technol* 1990;37(1–3):109–27.
- [50] Torquato S. *Random heterogeneous materials: microstructure and macroscopic properties*. New York: Springer-Verlag; 2002.
- [51] Sobczyk K, Kirkner DJ. *Stochastic modeling of microstructures*. New York: Springer; 2001.
- [52] Bochenek B, Pyrz R. Reconstruction of random microstructures—a stochastic optimization problem. *Comput Mater Sci* 2004;31–2:93–112.
- [53] Jeulin D. Random texture models for material structures. *Stat Comput* 2000;10(2):121–32.
- [54] Al-Ostaz A, Diwakar A, Alzabedeh KI. Statistical model for characterizing random microstructure of inclusion-matrix composites. *J mater Sci* 2007;42(16):7016–30.
- [55] Torquato S. Statistical description of microstructure. *Annu Rev Mater Res* 2002;32:77–111.
- [56] Jiao Y, Stillinger FH, Torquato S. A superior descriptor of random textures and its predictive capacity. *Proc Natl Acad Sci* 2009;106(42):17634–9.
- [57] Collins BC, Matous K, Ryppl D. Three-dimensional reconstruction of statistically optimal unit cells of multimodal particulate composites. *Int J Multiscale Comput Eng* 2010;8(5):489–507.
- [58] Torquato S. Optimal design of heterogeneous materials. *Annu Rev Mater Res* 2010;40:101–29.
- [59] Brinson HF, Brinson LC. *Polymer engineering science and viscoelasticity: an introduction*. New York, USA: Springer; 2007.
- [60] Watcharotone S, Wood CD, Friedrich R, Chen X, Qiao R, Putz K, et al. Interfacial and substrate effects on local elastic properties of polymers using coupled experiments and modeling of nanoindentation. *Adv Eng Mater* 2011;13(5):400–4.
- [61] Sun YY, Zhang ZQ, Moon KS, Wong CP. Glass transition and relaxation behavior of epoxy nanocomposites. *J Polym Sci Part B: Polym Phys* 2004;42(21):3849–58.
- [62] Ellison CJ, Torkelson JM. The distribution of glass-transition temperatures in nanoscopically confined glass formers. *Nature Mater* 2003;2(10):695–700.
- [63] Forrest JA, Dalnoki-Veress K. The glass transition in thin polymer films. *Adv Colloid Interfac Sci* 2001;94(1–3):167–96.